Journal of Sound and Vibration (1997) **205**(3), 265–273

AN INVESTIGATION ON FUNDAMENTAL FREQUENCIES OF LAMINATED CIRCULAR CYLINDERS GIVEN BY SHEAR DEFORMABLE FINITE ELEMENTS

G. SUN

School of Civil Engineering and Mechanics, Shanghai Jiao Tong University, Shanghai 200030, *People's Republic of China*

AND

P. N. BENNETT AND F. W. WILLIAMS

Division of Structural Engineering, Cardiff School of Engineering, University of Wales Cardiff, Cardiff CF2 3TB, Wales

(*Received* 29 *March* 1995, *and in final form* 9 *December* 1996)

The fundamental frequencies of laminated anisotropic circular cylindrical composite shells are investigated by using nine-noded isoparametric quadratic finite elements based on extended Sanders' first order shear deformable shell theory. Finite element (FE) results are presented for cylinders and compared with the exact results obtained by a computer program written by the authors and using the same shear deformable theory. Such comparisons are important to validate the FE method, because exact results can be obtained for only a few special lamination and boundary cases, and cannot be applied to cylinders with non-uniform structural or loading characteristics, holes, etc. In addition, results are compared with shear deformable results obtained by using numerous flat strips and the exact flat strip program VICONOPT. The agreement of the finite element results with the exact results is found to be good, including degenerated cases in which the shear stiffness approaches infinity: i.e., classical results. The effects of boundary conditions and lamination schemes on the fundamental frequency are also investigated. It is found that cylinders require many more elements than might be predicted from open shell panels in order to obtain any specified accuracy.

1. INTRODUCTION

The range of applications of composite materials in a variety of structures has increased rapidly and quite often includes laminated composite cylindrical shells.

In early research on laminated anisotropic thin shells the Kirchhoff–Love hypothesis was used: i.e., transverse shear deformation was neglected. This could lead to 30% or higher errors for deflections and frequencies. Reddy [1–3] extended Sanders' first order shear deformation theory [4] for doubly curved isotropic shells to cover laminated anisotropic shells, including finite element and exact results for the deflections and frequencies of simply supported, doubly curved laminated shells. Chandrashekhara [5] also presented numerical results for the free vibration of doubly curved laminated open shell panels based on the first order shear deformation model. While vibration problems for shells of revolution can certainly be analyzed more efficiently by using one-dimensional semi-analytical axisymmetric elements, in engineering applications the load and/or pattern

0022–460X/97/330265 + 09 $25.00/0/sv960975

of openings and/or distribution of attached masses are often asymmetric, so that discretization of the entire surface is required, using two dimensional elements.

Published results using Reddy's theory, including those cited above, only demonstrate its efficiency for open shell panels. Therefore the present paper investigates its efficiency for the vibration of laminated cylinders by comparing results obtained from two computer codes developed for this paper. These both use Reddy's theory [3], but differ because one uses finite elements while the other is exact, but can only solve a limited range of problems.

To enable the comparisons to be made, a nine-noded shear deformable finite element model is developed, which has nodes at its corners, the mid-lengths of its sides and its centre. To confirm the reliability of this finite element and of the associated computer codes (which are used for all of the FEM results presented), numerical results are first compared with exact solutions for cross-ply spherical and cylindrical shell panels and for antisymmetric angle-ply flat laminated plates. Finite element results obtained for the fundamental frequency of various simply supported laminated cylinders are then compared with exact first order shear deformable theory results, degenerated results obtained by artificially assuming high transverse shear modulus for the laminates, and Donnell type classical solutions. Additionally, it is shown that the exact results and the corresponding degenerated results coincide very well with, respectively, shear deformable and classical results obtained by using numerous flat strips and the exact flat strip program VICONOPT [6, 7]. Finally, the influence of boundary conditions and laminate configurations on the fundamental frequencies of laminated cylinders are investigated.

2. FINITE ELEMENT FORMULATION

Let the x–y surface of the orthogonal curvilinear shell co-ordinates coincide with the mid-surface of a composite shell, so that the z-axis is normal to it; see Figure 1. The shell consists of a finite number of plies, with the major material axis lying in the x–y surface with an arbitrary inclination to the x-axis. In first order shear deformable shell theory, normals to the mid-surface of the shell before deformation are assumed to remain straight, but not necessarily normal, after deformation, to give the displacement field as [3]

$$\bar{u} = (1 + z/R_1)u + z\phi_x, \qquad \bar{v} = (1 + z/R_2)v + z\phi_y, \qquad \bar{w} = w, \tag{1}$$

where (see Figure 1) $\bar{u}$, $\bar{v}$ and $\bar{w}$ are the displacements of a point (x, y, z) parallel to the co-ordinates x, y and z respectively; similarly u, v and w are the displacements of a point $(x, y, 0)$ on the middle surface; ϕ_x and ϕ_y are the rotations of the line normal to the middle surface about the y- and x-axis, respectively; and R_1 and R_2 are the principal radii of

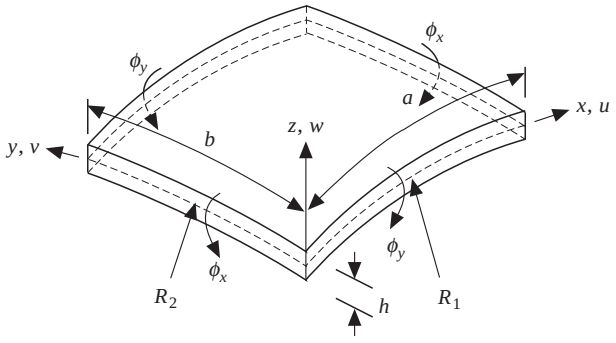

Figure 1. The geometry and displacements of a laminated doubly curved shell panel.

curvature of the middle surface. The strain displacement relations of the shear deformable doubly curved shell element are

$$\varepsilon_1 = \varepsilon_1^0 + zk_1, \qquad \varepsilon_2 = \varepsilon_2^0 + zk_2,$$
$$\varepsilon_4 = \varepsilon_4^0, \qquad \varepsilon_5 = \varepsilon_5^0, \qquad \varepsilon_6 = \varepsilon_6^0 + zk_6, \tag{2}$$

where ε_i ($i = 1, 2, 6$) are the in-plane strains and ε_4 and ε_5 are the transverse shear strains at the point (x, y, z), and

$$\varepsilon_1^0 = \partial u/\partial x + w/R_1, \qquad \varepsilon_2^0 = \partial v/\partial y + w/R_2, \qquad \varepsilon_4^0 = \phi_y + \partial w/\partial y - v/R_2,$$
$$\varepsilon_5^0 = \phi_x + \partial w/\partial x - u/R_1, \qquad \varepsilon_6^0 = \partial u/\partial y + \partial v/\partial x, \qquad k_1 = \partial\phi_x/\partial x, \qquad k_2 = \partial\phi_y/\partial y,$$
$$k_6 = \partial\phi_x/\partial y + \partial\phi_y/\partial x - C_0(\partial v/\partial x - \partial u/\partial y), \qquad C_0 = (1/2)\{(1/R_1) - (1/R_2)\}.$$

Applying Hamilton's principle to the Lagrangian variational of the shell yields

$$\int_\Omega [N_1\delta\varepsilon_1^0 + N_2\delta\varepsilon_2^0 + N_6\delta\varepsilon_6^0 + M_1\delta k_1 + M_2\delta k_2 + M_6\delta k_6 + Q_1\delta\varepsilon_5^0$$
$$+ Q_2\delta\varepsilon_4^0 + (P_1\ddot{u} + P_2\ddot{\phi}_x)\,\delta u + (P_3\ddot{v} + P_4\ddot{\phi}_y)\,\delta v + I_1\ddot{w}\,\delta w$$
$$+ (I_3\ddot{\phi}_x + P_2\ddot{u})\delta\phi_x + (I_3\ddot{\phi}_y + P_4\ddot{v})\delta\phi_y]\,\mathrm{d}x\,\mathrm{d}y = 0, \tag{3}$$

where Ω is the area of the middle surface, the N_i, M_i and Q_i are the stress, moment and transverse shear force resultants given by

$$(N_i, M_i) = \sum_{j=1}^{p} \int_{z_j}^{z_{j+1}} \sigma_i(1, z)\,\mathrm{d}z, \qquad i = 1, 2, 6,$$

$$(Q_1, Q_2) = \sum_{j=1}^{p} \int_{z_j}^{z_{j+1}} (K_1^2\sigma_5, K_2^2\sigma_4)\,\mathrm{d}z, \tag{4}$$

the σ_i ($i = 1, 2, 6$) are the in-plane stresses and σ_4 and σ_5 are the transverse shear stresses, z_j and z_{j+1} denote the surfaces of the jth ply, p is the number of plies in the shell, $K_1 = K_2 = 5/6$ are the shear correction factors, the P_i are defined as

$$P_1 = I_1 + 2I_2/R_1, \qquad P_2 = I_2 + I_3/R_1, \qquad P_3 = I_1 + 2I_2/R_2, \qquad P_4 = I_2 + I_3/R_2, \tag{5}$$

and

$$(I_1, I_2, I_3) = \sum_{j=1}^{p} \int_{z_j}^{z_{j+1}} \rho^{(j)}(1, z, z^2)\,\mathrm{d}z$$

where $\rho^{(j)}$ is the mass density of the jth ply. The stress resultants are related to the strains by

$$N_i = A_{ij}\varepsilon_j^0 + B_{ij}k_j, \quad M_i = B_{ij}\varepsilon_j^0 + D_{ij}k_j, \qquad i, j = 1, 2, 6,$$
$$Q_1 = A_{45}\varepsilon_4^0 + A_{55}\varepsilon_5^0, \quad Q_2 = A_{44}\varepsilon_4^0 + A_{45}\varepsilon_5^0, \tag{6}$$

where the A_{ij}, B_{ij} and D_{ij} are the stiffness coefficients of the laminate, so that

$$(A_{ij}, B_{ij}, D_{ij}) = \sum_{k=1}^{p} \int_{z_{k-1}}^{z_k} Q_{ij}(1, z, z^2)\,\mathrm{d}z, \qquad i, j = 1, 2, 6,$$

the shear stiffness coefficients are

$$(A_{44}, A_{45}, A_{55}) = \sum_{k=1}^{p} \int_{z_{k-1}}^{z_k} (K_1^2 Q_{44}, K_1 K_2 Q_{45}, K_2^2 Q_{55})\, \mathrm{d}z,$$

and the Q_{ij} ($i, j = 1, 2, 6$, and $i, j = 4, 5$) are the stiffnesses of a ply in the material principal co-ordinates.

Typical nine-noded quadratic isoparametric finite elements are used to discretize the middle surface of the shell, with the displacements (u, v, w, ϕ_x, ϕ_y) interpolated over the shell element by shape functions ψ_j ($j = 1, 9$) such that

$$u = \sum_{j=1}^{9} u^j \psi_j(x, y), \qquad v = \sum_{j=1}^{9} v^j \psi_j(x, y), \qquad w = \sum_{j=1}^{9} w^j \psi_j(x, y),$$

$$\phi_x = \sum_{j=1}^{9} \phi_x^j \psi_j(x, y), \qquad \phi_y = \sum_{j=1}^{9} \phi_y^j \psi_j(x, y), \tag{7}$$

where u^j, v^j, w^j, ϕ_x^j, and ϕ_y^j are nodal values of u, v, w, ϕ_x and ϕ_y, respectively.

Substitution of equation (7) into equation (3) gives the equations for the element as

$$[\mathbf{K}]\{\mathbf{d}\} + [\mathbf{M}]\{\ddot{\mathbf{d}}\} = \mathbf{0}, \tag{8}$$

where $\mathbf{d}$ is the vector of node displacements and [**K**] and [**M**] are, respectively, the element stiffness and mass matrices. To avoid the shear locking effect, reduced integration is used to evaluate the coefficients associated with transverse shear energy terms in the stiffness matrix, while full integration is used to evaluate its other coefficients and all of the coefficients in the mass matrix. For free vibration, $\mathbf{d}$ takes the form $\mathbf{d}(t) = \mathbf{d}\, \mathrm{e}^{\mathrm{i}\omega t}$. Assembly of the element equations gives the eigenvalue problem

$$([\mathbf{K}] - \omega^2[\mathbf{M}])\{\mathbf{d}\} = \mathbf{0}, \tag{9}$$

from which the fundamental frequency is found by using subspace iteration [8].

3. NUMERICAL RESULTS

The finite element results presented were obtained on a VAX computer, using single precision arithmetic. In every case, the entire region of the shell was discretized without making use of any preconceived assumption of symmetry of the vibration mode with respect to the coordinates. The ply material properties assumed for all examples, in the usual notation, were $E_{11} = 25E_{22}$, $G_{12} = G_{13} = 0{\cdot}5E_{22}$, $G_{23} = 0{\cdot}2E_{22}$, $\nu_{12} = 0{\cdot}25$ and mass density $\rho = 1{\cdot}0$. The first three examples were used to test the validity of the formulation and computer code, as follows.

Examples 1 and 2 were to find the fundamental frequency of two types of square cross-ply shell panels with side length a; namely, a spherical shell panel and a cylindrical shell panel. For both examples the alternative lay-ups (0/90) and (0, 90, 90, 0) were used, the thickness h was $0{\cdot}1a$ and the radius of curvature R ranged between a and near to infinity: i.e., effectively a flat plate. The boundary conditions were SS2, i.e.,

$$u = w = \phi_x = 0 \quad \text{at } y = 0, a, \qquad v = w = \phi_y = 0 \quad \text{at } x = 0, a, \tag{10}$$

the stiffness coefficients satisfy

$$A_{16} = A_{26} = B_{16} = B_{26} = D_{16} = D_{26} = A_{45} = 0 \tag{11}$$

and the Euler equations of the variational equation (3) admit an exact solution when the spatial variation of displacements takes the form [3]

$$u(x, y) = U_{mn} \cos \alpha x \sin \beta y, \qquad v(x, y) = V_{mn} \sin \alpha x \cos \beta y,$$
$$w(x, y) = W_{mn} \sin \alpha x \sin \beta y, \qquad \phi_x(x, y) = \Phi_{xmn} \cos \alpha x \sin \beta y,$$
$$\phi_y(x, y) = \Phi_{ymn} \sin \alpha x \cos \beta y, \tag{12}$$

where $\alpha = m\pi/a$ and $\beta = n\pi/a$. For both examples, the numbers of half-waves m and n in the x and y directions for the vibration mode associated with the fundamental frequency were always $m = n = 1$. The FEM results obtained by using a 4×4 mesh all agreed to an accuracy of 0·3% or better with the results given by the authors' exact code, which was based on equation (12). The results from this exact code also agreed very well with the exact results given by Reddy [2].

Example 3 was chosen because antisymmetric angle-ply laminated shells with simply supported boundary conditions do not admit exact solutions. Therefore Example 3 consists of the degenerate case of an antisymmetric angle-ply shell with its radii of curvature approaching infinity such that it approximates a square flat plate. The FEM results for its fundamental frequency were compared with corresponding exact flat plate results for a $(+\theta, -\theta, +\theta, -\theta)$ lay-up, for values of θ in the range $0 \leqslant \theta \leqslant 45^\circ$. The boundary conditions were SS1, i.e.,

$$v = w = \phi_x = 0 \quad \text{at } y = 0, a \qquad u = w = \phi_y = 0 \quad \text{at } x = 0, a, \tag{13}$$

the stiffness coefficients satisfy

$$A_{16} = A_{26} = B_{16} = B_{26} = D_{16} = D_{26} = A_{45} = 0, \tag{14}$$

and the Euler equations of the variational equation (3) admit an exact solution when the spatial variation of displacements takes the form [3]

$$u(x, y) = U_{mn} \sin \alpha x \cos \beta y, \qquad v(x, y) = V_{mn} \cos \alpha x \sin \beta y,$$
$$w(x, y) = W_{mn} \sin \alpha x \sin \beta y, \qquad \phi_x(x, y) = \Phi_{xmn} \cos \alpha x \sin \beta y,$$
$$\phi_y(x, y) = \Phi_{ymn} \sin \alpha x \cos \beta y. \tag{15}$$

The FEM results obtained by using a 4×4 mesh agreed to within 0·15% with those obtained from the authors' exact code, which used equation (15). The results from this exact code also agreed well with those given by Reddy [3].

So far, the finite element method results have coincided very well with the exact results, because the fundamental mode shapes for square plates and shell panels often have a single half-wave in both directions. The agreement is less good for Example 4, as follows.

Example 4 is the following circular cylinder problem; see Figure 2. The middle surface is the reference surface, the origin of the co-ordinates is at one of its ends, and x, y and z are in the axial, circumferential and normal directions, respectively. The length, wall thickness and radius of the cylinder are, respectively, L, h and R_2. The FEM results were compared with the exact dimensionless results for the simply supported laminated circular cylindrical shell, with the non-dimensional circular frequency defined as $\bar{\omega} = \omega(R_2^2/h)\sqrt{(\rho/E_{22})}$.

An exact solution exists only for circular cylindrical shells with laminate stiffness coefficients satisfying equation (11), and with SS2 end conditions: i.e., $v = w = \phi_y = 0$ at $x = 0$ and L. It is obtained by assuming that the displacement field has the form of equation (12) with $\alpha = m\pi/L$ and $\beta = \bar{n}y/R_2$, where m is the number of half-waves in the x direction while $\bar{n}$ is the number of full waves round the circumference. Substituting

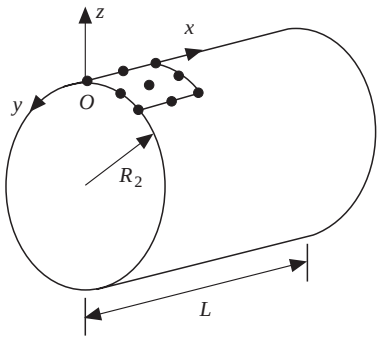

Figure 2. The geometry of a laminated circular cylindrical shell. $L = 2R_2$ for all cylinder results presented.

equation (12) into the Euler equation, which can be derived from the variational equation (3), yields a set of five linear algebraic eigenequations in terms of the unknown amplitudes U_{mn}, V_{mn}, W_{mn}, Φ_{xmn} and Φ_{ymn}, from which the exact fundamental frequency can be obtained, as shown in detail by Reddy [3]. The authors' exact code used this method.

Note that in the FEM formulation the SS2 end conditions do not exclude a rigid body movement of the circular cylinder in the x direction. Therefore the exact solution was obtained first, to find the wavenumbers m and $\bar{n}$ associated with the fundamental frequency. Then, for the FEM results, the SS2 end conditions were supplemented by the additional boundary conditions

$$u(0, y) = 0, \quad u(L, y) = 0, \qquad \text{when } y = 2i\pi R_2/\bar{n}, \quad i = 0, 1, 2, \ldots, \bar{n} - 1, \tag{16}$$

which are consistent with the exact solution because they are implied by its displacement field: i.e., by equation (12).

In order to examine the effects of shear deformation, a degenerated case of Sanders' first order theory was used in which the transverse shear moduli G_{13} and G_{23} were multiplied by 10^4: i.e., $G_{13} = 0{\cdot}5 \times 10^4 E_{22}$ and $G_{23} = 0{\cdot}2 \times 10^4 E_{22}$. Thus transverse shear deformation was prevented and so the Kirchhoff hypothesis is implied.

In Table 1 are compared, for $R_2 = 0{\cdot}5L$, the non-dimensional fundamental frequencies of the FEM solutions with exact results from the authors' code, degenerated solutions and Donnell type classical thin shell results (see reference [9]), for six alternative lay-ups and two alternative wall thicknesses. The first three lay-ups are typical cross-ply laminates, while the next three are assumed to have an infinite number of $+\theta$, $-\theta$, $+\theta$, $-\theta$, ..., plies of infinitesimal thickness, so that they satisfy equation (11). The finite element model had either three or four elements in the axial direction and 10–20 elements for each wave in the circumferential direction; see the column headed "Mesh" in Table 1.

Example 5 compares the exact solutions given in the bottom half of Table 1 and the corresponding degenerated results with, respectively, shear deformable and classical results obtained by VICONOPT. VICONOPT is an efficient design code [6] which was developed on the basis of the Wittrick and Williams theory and algorithms [7]. Its theory provides an exact solution for the buckling load and vibration frequency of structures which are assumed to consist of a series of long flat strips rigidly connected together at their longitudinal edges and simply supported at their ends. In Table 2 the frequencies were calculated by modelling the cylinder as a polygon with a large number of sides and then increasing the number of sides until the solution converged. The VICONOPT shear deformable results, which used the theory of Anderson and Kennedy [10], clearly coincide

TABLE 1

Results for the fundamental frequency $\bar{\omega}$ *of Example* 4; *the error columns are relative to the exact results*

		Shear deformable				Degenerated results		Donnell's theory	
Lamination	$m, \bar{n}$	Exact	FEM	Mesh	Error (%)		Error (%)		Error (%)
$h = 0{\cdot}04\ R_2$									
0, 90	1, 3	9·510	9·526	4 × 60	0·17	9·500	−0·11	10·579	11·24
90, 0, 90, 0	1, 3	11·317	11·331	4 × 60	0·13	11·474	1·39	12·606	11·39
90, 0, 0, 90	1, 2	12·603	12·652	3 × 30	0·38	12·631	0·22	14·535	15·33
±30*	1, 4	15·082	15·110	4 × 60	0·18	15·338	1·70	16·672	10·54
±45*	1, 3	13·372	13·417	4 × 60	0·34	13·516	1·08	15·802	18·17
±60*	1, 3	12·142	12·179	4 × 60	0·31	12·432	2·39	14·548	19·82
$h = 0{\cdot}1\ R_2$									
0, 90	1, 2	5·115	5·142	3 × 20	0·54	5·146	0·61	6·228	21·76
90, 0, 90, 0	1, 2	5·910	5·924	3 × 30	0·24	6·014	1·76	7·116	20·41
90, 0, 0, 90	1, 2	6·004	6·019	4 × 30	0·25	6·235	3·85	7·870	31·08
±30*	1, 3	9·644	9·661	4 × 45	0·18	10·235	6·13	10·879	12·81
±45*	1, 3	8·500	8·516	4 × 45	0·19	9·632	13·32	11·930	40·35
±60*	1, 2	6·912	6·931	4 × 40	0·27	7·112	2·89	9·829	42·20

* The number of plies is infinite.

quite well with Sanders' first order shear deformable results, while the VICONOPT classical results coincide even better with the degenerated ones.

Example 6 uses FEM results to demonstrate the effect on the fundamental frequency of changing the end conditions of laminated cylindrical shells with $L/R_2 = 2$, $h/R_2 = 0{\cdot}02$ and six alternative lay-ups; see Table 3. The SS3 and clamped end conditions at $x = 0$ and L were, respectively, $u = v = w = \phi_y = 0$ and $u = v = w = \phi_x = \phi_y = 0$. Numerical experiments were performed with different grid sizes to ensure that the results presented are sufficiently accurate.

Finally, Example 7 examines the effect on the fundamental frequency of a clamped cylinder of changing the lay-up detail; see Figure 3. It gives the non-dimensional

TABLE 2

VICONOPT *shear deformable and classical results for the fundamental frequencies* $\bar{\omega}$ *of Example* 5 *compared with results from the authors' exact code based on Reddy's theory* [3]; *the difference columns are relative to the exact and degenerated results, respectively*

$h = 0{\cdot}1\ R_2$, lay-up	Exact	VICONOPT shear	Difference (%)	Degenerated	VICONOPT classical	Difference (%)
0, 90	5·115	5·103	−0·23	5·146	5·132	−0·27
90, 0, 90, 0	5·910	5·880	−0·51	6·014	6·010	−0·07
90, 0, 0, 90	6·004	5·956	−0·80	6·235	6·242	0·11
±30*	9·644	9·606	−0·39	10·235	10·184	−0·50
±45*	8·500	8·430	−0·82	9·632	9·624	−0·08
±60*	6·912	6·886	−0·38	7·112	7·102	−0·14

* The number of plies is infinite.

TABLE 3

FEM *results for Example* 6; *i.e., for the fundamental frequency* $\bar{\omega}$ *for* SS2, SS3 *and clamped circular cylinders with* $h = 0{\cdot}02\ R_2$

Lamination (degrees)	Boundary conditions		
	SS2	SS3	Clamped
0, 90	15·188	16·662	16·914
90, 0, 90, 0	18·359	18·870	20·349
90, 0, 0, 90	19·503	20·246	20·944
± 30*	20·681	28·184	29·674
± 45*	18·765	28·232	29·142
± 60*	17·604	26·126	26·546

* The number of plies is infinite.

fundamental frequencies for lay-ups with two, four or eight identical orthotropic plies with alternating alignments of $+\theta$ and $-\theta$, for all possible values of θ.

4. DISCUSSION AND CONCLUSIONS

The first three examples show that the FEM presented is quite accurate and efficient for analysis of open shell panels and plates. They also validate the authors' computer codes for both exact and FEM results.

The FEM results of Example 4 indicate that the number of elements needed in the circumferential direction of a cylinder for relatively high accuracy is 5–10 for each half-wave, whereas four elements per half-wave in each direction are usually sufficient for practical open shell panels. The degenerated results show that the shear deformation effect was not very significant for a cylinder with $h = 0{\cdot}04\ R_2$ but, depending on lamination scheme, became more so for a thicker cylinder with $h = 0{\cdot}1\ R_2$. Donnell type thin shell theory would not be expected to be very accurate for this type of problem and predicted much higher frequencies, with errors ranging from 11% to 42% compared with exact first

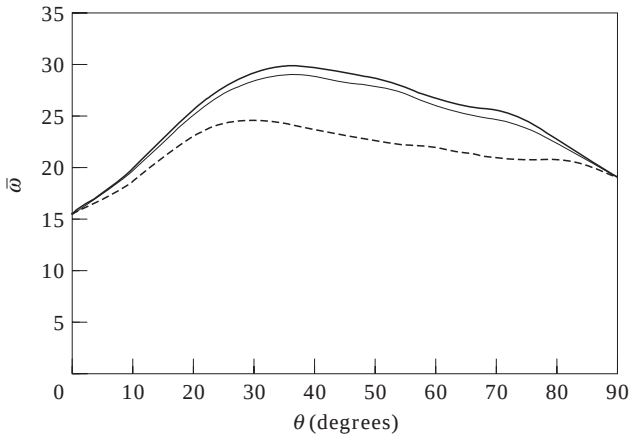

Figure 3. The non-dimensional fundamental frequency for three lamination schemes, for a clamped cylinder $h = 0{\cdot}02\ R_2$. – – – –, $+\theta, -\theta$; ——, $+\theta, -\theta, +\theta, -\theta$; ——, $+\theta, -\theta, \ldots$, eight-layer.

order Sanders' theory. Therefore, Donnell type theory is inadequate for vibration analysis of moderately thick composite cylinders.

The shear locking phenomenon in FEM analysis has been successfully circumvented by using a reduced integration scheme, and the error caused by finite element modelling based on first order shear deformable theory meets engineering requirements.

Because of Rayleigh's theorem, the fundamental frequency of any cylinder must increase as its boundary constraints are changed from SS2 to SS3 and then to clamped, since the changes involve adding constraints without removing any. The results of Example 6 listed in Table 3 satisfy this requirement and show that the increases are fairly small for cross-ply laminated cylinders, whereas the increase between the SS2 and SS3 cases is large for cylinders composed of an infinite number of $\pm\theta$ plies.

Finally, the results of Example 7 shown in Figure 3 demonstrate that the fundamental frequency is increased significantly by increasing the number of layers while keeping the total thickness of the cylinder constant, as also occurs for laminated flat plates.

ACKNOWLEDGMENTS

The financial support of the British Council and of the Advanced Chinese Engineering Centre of the University of Wales Cardiff is gratefully acknowledged.

REFERENCES

1. J. N. Reddy 1982 *Fibre Science and Technology* **17**, 9–24. Bending of laminated anisotropic shells by a shear deformable finite element.
2. J. N. Reddy 1984 *Journal of the Engineering Mechanics Division*, *American Society of Civil Engineers* **110**, 794–809. Exact solutions of moderately thick laminated shells.
3. J. N. Reddy 1986 *Energy and Variational Methods in Applied Mechanics*. New York: John Wiley.
4. J. L. Sanders Jr. 1959 *NASA Technical Report R*-24. An improved first-approximation theory for thin shells.
5. K. Chandrashekhara 1989 *Computers and Structures* **33**, 435–440. Free vibrations of anisotropic laminated doubly curved shells.
6. R. Butler and F. W. Williams 1992 *Computers and Structures* **43**, 699–708. Optimum design using VICONOPT, a buckling and strength constraint program for prismatic assemblies of anisotropic plates.
7. W. H. Wittrick and F. W. Williams 1974 *International Journal of Mechanical Sciences* **16**, 209–239. Buckling and vibration of anisotropic or isotropic plate assemblies under combined loadings.
8. K. J. Bathe 1982 *Finite Element Procedures in Engineering Analysis*. Englewood Cliffs, New Jersey: Prentice-Hall.
9. R. M. Jones and H. S. Morgan 1975 *American Institute of Aeronautics and Astronautics Journal* **13**, 664–671. Buckling and vibration of cross-ply laminated circular cylindrical shells.
10. M. S. Anderson and D. Kennedy 1993 *American Institute of Aeronautics and Astronautics Journal* **31**, 1963–1965. Transverse shear deformation in exact buckling and vibration of composite plate assemblies.